Comparative study of afterpulsing behavior

Abdul W. Ziarkash,[1] Siddarth Koduru Joshi,[2, a)] Mario Stipčević,[3] and Rupert Ursin[4, b)]
[1)] *Institute for Quantum Optics and Quantum Information, Austrian Academy of Sciences Vienna A-1090*
[2)] *Institute for Quantum Optics and Quantum Information, Austrian Academy of Sciences, Vienna A-1090*
[3)] *Ruder Boskovic Institute, Center of Excellence for Advanced Materials and Sensors and Division of Experimental Physics, Zagreb 10000, Croatia*
[4)] *Institute for Quantum Optics and Quantum Information, Austrian Academy of Sciences, Vienna A-1090*
Vienna Center for Quantum Science and Technology (VCQ).

(Dated: 17 January 2017)

PACS numbers: 03.67.Dd, 03.67.Hk, 85.60.Gz, 06.20.fb, 07.60.-j, 87.64.-t,
Keywords: Afterpulse, Avalanche photodiode, APD, Single photon detection

arXiv:1701.03783v1 [physics.ins-det] 12 Jan 2017

Single-photon detectors, like Avalanche Photo Diodes (APDs), have a great importance in many fields like quantum key distribution, laser ranging, florescence microscopy, etc. Afterpulsing is a typical non ideal behavior of APDs, operated in Geiger mode, which adversely affects any application which measures the number or timing of detection events. Several conflicting studies have tried to model afterpulsing behavior and link it to fundamental semiconductor physics[3,7,8,13,15,17,25]. Here we describe experiments we performed on at least 2 different detectors from 3 manufacturers, all commonly used in quantum optics setups. We report on the timing structure of the counts. By fitting different models to these data, we found statistically significant differences between the detectors used. Furthermore, we report on the presence of high order afterpulses which are not accounted for in any of the standard models of afterpulse behavior. This might have significant implication e.g. in quantum key distribution systems, as the modeling of the devices in use will have to be part of the security analysis for some systems[9,10]. Significant differences between manufacturers and even between seemingly identical detectors of the same make and batch suggest that every individual detector needs to be calibrated. We describe a reliable procedure to perform such a calibration and present our findings on three different commercial products.

I. INTRODUCTION

Applications of single-photon detectors, which focus on the timing of a very weak optical signal, mostly use Avalanche Photo Diodes (APDs) operated above their breakdown voltage in Geiger mode. Such as in photonics quantum processing tasks, laser ranging, fluorescence microscopy, neural imaging with blood flow tomography, contrast-enhanced MRI, two-photon luminescence imaging, astronomical telescopes, etc.[5,6,11,12,19,26,28]. They are widely manufactured and sold by many different companies and as such exhibit different properties/behavior. To efficiently and accurately perform these experiments we must account for all non-ideal behavior of the detectors used[1,4]. This is especially true for sensitive applications like quantum communication, because the security of any real world implementation (i.e. with a high transmission loss) depends on the devices used. Hence the precise modeling/characterization of the non ideal behavior of single photon detectors (and all other components of the quantum communication device) are critical for practical security proofs.

An ideal single-photon detector generates one and only one electric pulse for every incident photon. However, in a real detector, it is possible that a single incident photon results in more than one electrical pulse per incident photon. This is known as afterpulsing.[1] In this work we define an "afterpulse" as any pulse in addition to and following the detection event caused by an incident photon, regardless of its etiology. This behavior has been extensively studied due to its importance in semiconductor physics in general. It has been suggested that afterpulsing can be linked to charges trapped in the deep levels of the semiconductor's band structure and released at a later time[3] as well as to an artifact of the electronics like unsuccessful quenching[2] or twilighting[22,24,29] (i.e. a detection event towards the end of the dead time).

Afterpulsing has different implications, depending on the application of the detector used. It can result in an overestimation of the total count rate by up to 10 % as well as a reduction of the duty cycle and detection efficiency due to the increased dead times. In fluorescence microscopy it could lead to an overestimation of the concentration of fluorophores. In quantum communication the overestimation of coincidence events leads to larger Quantum Bit Error Ratio (QBER). Afterpuls-

[a)] Electronic mail: Siddarth.Koduru.Joshi@oeaw.ac.at.
[b)] Electronic mail: Rupert.Ursin@oeaw.ac.at.

ing can also adversely affect security[16] and hence part of the security analysis of the quantum key distribution system. Afterpulsing poses also a significant problem to the measurement of photon arrival times both in quantum communication protocols as well as for laser ranging. Hence a proper characterization of the afterpulse behaviour could improve the accuracy of several measurements in meterology in general. Further, studying the afterpulses could lead to a better understanding of the underlying mechanism within the semiconductor.

Several previous works have attempted to characterize the afterpulse behavior and fit the results to various models[3,7,8,13,15,17,25]. Worryingly, these papers do not agree on the most suitable model describing the statistics of the arrival times. All these studies have focused on one make/manufacture of detector at a time. In this work we take a more comprehensive approach and perform a comparative study on 3 different makes of APDs (for each make we compare 2 individual detectors with almost consecutive serial numbers). We test the universality of the various theoretical models and attempt to resolve the conflicts raised by these works. To do so we eschew the common practice of studying the timing auto-correlation of the APD signals in favor of the more comprehensive timing cross-correlation between the emission of a photon and all the following APD signals. We describe this procedure in Section II. We then fit to the various standard models described below and compare these fits in Section III A. Due to our use of cross-correlations we were also able to detect higher orders of afterpulses which we present in Section III B and finally in Section III C we discuss the corrections that can be applied.

The characteristic decay of the afterpulse probability was sometimes thought to depend on the deep level in which the charge is trapped. Initial models[3,7,8,18,30] considered the decay from several distinct deep levels and proposed the "multiple exponential model" where the afterpulsing probability ($P_{exp}(t)$) at a time t is given by:

$$P_{exp}(t) = \sum_k A_k e^{-\frac{t}{\tau_k}} + d, \tag{1}$$

where τ_k and A_k is the de-trapping lifetime and amplitude factor for the k^{th} deep level, and d is the offset due to noise counts.

Furthermore[14,15] considered a continuum of deep levels, in InGaAs and InP detectors, that could trap a charge and found that the "power law" was a good empirical fit. Here the afterpulse probability ($P_{pow}(t)$) is given by:

$$P_{pow}(t) = A \cdot t^{-\lambda} + d, \tag{2}$$

where λ is a effective decay constant and A is the the initial afterpulse probability.

In an another attempt to create a more physically meaningful model[13] derived the "hyperbolic Sinc model" from the Arrhenius law (once more assuming a continuum of levels), where the afterpulse probability ($P_{sinc}(t)$) is given by:

$$P_{sinc}(t) = 2 \cdot A \cdot \frac{\sinh(\Delta \cdot t)}{t} \cdot e^{-\gamma \cdot t} + d, \tag{3}$$

where Δ and γ are both functions of the minimum and maximum energies of the deep levels in which charges may be trapped.

In this paper, we compare the above three standard mathematical models (see Equations 1, 2 and 3) with the measured behavior of several different single photon counting APDs (SPCM-AQ4C from PerkinElmer, SPCM-NIR from Excelitas and τ-SPAD-fast from Laser Components). We show that none of these canonical models are universal and vary between makes of detectors. We also report on the presence of several higher order afterpulses. An investigation of the region of reduced detection efficiency called the "dead-time" found between the signal pulse and the afterpulse shows yet another characteristic variation between makes of detectors, which is not part of the models used so far.

II. EXPERIMENTAL SETUP

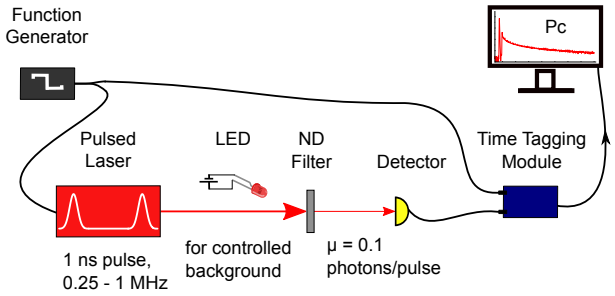

FIG. 1: A 798 nm laser is used to generate pulses with a 1 ns pulse width and various repetition rates between 0.25 to 1 MHz. We use Neutral Density (ND) filters to attenuate the laser pulse, incident on the active area of the APDs, until we have $\ll 1$ detected photon per laser pulse (approximately corresponding to a mean photon number of 0.1 per pulse). We use a time tagging module (TTM8000) with a resolution of 82.3 ps to record the trigger for the laser pulse (Channel 1) and the photon detection event (Channel 2). This data is stored on a computer and a software computes the temporal cross-correlation histogram ($g^{(2)}$) with 1 ns bin width. The LED shown was only used to obtain the results shown in Section III C.

The general scheme of the setup used for the experiments is shown in Figure 1. A function-generator triggers a 789 nm laser with a repetition rate of 0.25 to 1 MHz kHz. The emitted light pulse of $\approx$ 1 ns length gets attenuated in a neutral attenuator to <0.1 photons per pulse on average and arrives at the active area of the respective detector in use. The arrival time at the detector and

the trigger from the function generator are individually sent to a time-tagging-module (TTM). We then calculated the temporal cross-correlation histogram ($g^{(2)}$) between those two signals using a bin width of 1 ns. We normalize to the number of laser pulses to obtain the pulse probability per bin and integrate over the entire peak to obtain the total pulse probability. To ensure that our results are not skewed by an individual "faulty" detector we tested at least 2 detectors of each type (same manufacturer's model number with nearly consecutive serial numbers) all of similar ages.

We consider the first event arriving at the TTM, after a given laser pulse to be the "detection pulse" which stems from the real photon impinging on the active area of the detector. Any detection event after that, but before the next laser pulse, should be due to to either afterpulsing or noise. Consequently, we do not differentiate between an afterpulse due to processes in the semiconductor diode from those due to secondary avalanches caused by the quenching circuit. This is typical of most applications of these detectors ranging from (quantum) optics experiments to fluorescence microscopy.

We fit each of the standard models (see Equations 1, 2 and Equation 3) to the tail of the afterpulse as seen in the $g^{(2)}$ obtained for each different APD. Figure 2 shows the resultant fits as well as the residuals.

All current models of afterpulsing discussed, concern the timing structure of the afterpulse tail. An ideal model of a detector should include its entire behaviour including the duration of the dead time, the jitter and the rising edge of the afterpulse peak. As in all previous publications mentioned above, we then isolate the peak (due to afterpulses) and its tail in time. The tail of the afterpulse of all APDs are shown in Figure 2 after normalization and accidentals correction have been applied (as discussed in Section III C). We define the total afterpulse probability to be the sum total of the afterpulse probability in each bin of the corrected $g^{(2)}$ histogram for a duration of 900 ns[31]. Regardless of the model, in order to obtain a good fit we had to ignore the first two points of the afterpulse tail.

III. RESULTS

A. Comparison of afterpulsing models

We observed a wide variation between different detectors. We tested 2 to 3 identical (in terms of make, model number and year of purchase) detectors from each of three manufacturers. We saw a drastic change in the total afterpulse probability between otherwise identical detectors. The total afterpulse probability of τ-SPAD-fast with serial number 01019917 was 5.1± 0.003 % and that with serial number 01019920 was 8.5± 0.002 % (see Table I). However, each identical detectors, had nearly the same fitting parameters for the same model. The only significant difference was the amplitude factor A.

On the whole, the power model had the most consistent good fit and the hyperbolic Sinc model the worst. Unlike the hyperbolic Sinc model, the power model approximates the experimental data more accurately independent of the APD used (AQ4C, SPCM-NIR, τ-SPAD-fast). [13] showed that the hyperbolic sinc model was better than the power model using id100-MMF50 APD module from idQuantique, we were unable to duplicate those results with any of our detectors.

One can clearly see in Figure 2 that the Power model is fitting the entire range of the tail better than the Hyperbolic sinc model. The goodness of the fits can be quantitatively compared using the residuals seen in Figure 2 which are well within the ± 2 standard deviation range (shown in red) for the power model but not for the hyperbolic sinc model.

Power model as a simple analytic model function leads to some good results (as seen in Figure 2). The power model was primarily shown to be effective for InGaAS and InP detectors[14,15,23] and we now show that it is a reasonably good model for the different types of Si detectors we tested. However, it's estimated parameters gives a rather loose description of the physical origin of afterpulses. A truly good model should be able to predict the behavior of the entire tail region. The power model only provides a suitable fit if the beginning of the afterpulse tail is ignored. Further,[13] showed that this model was not suitable for his idQuantique id100-MMF50 modules.

The multiple exponential model provides a good fit when $k \geqslant 5$ and is slightly better than the power model for the SPCM-AQ4C detector. It is nearly commensurate with the power model for the τ-SPAD. For the SPCM-NIR, the exponential model gives a good fit only when we ignore the higher order afterpulse peaks (which are discussed in Section III B). We observed that it was possible to get different fits of almost the same quality with different characteristic times (τ_k also called the de-trapping times) depending on the number of exponentials used. Thus, upon examining the fitting procedure we concur with[15] who state that "It is evident from this whole fitting procedure that the extracted values for the de-trapping times depend entirely on number of exponentials in the model function and the range of hold-off times used in the data set."

In case of the hyperbolic sinc model, we consistently obtain unsuitable fits to our experimental data. However, the behavior of detectors from other manufacturers may be better described by this model[13].

Afterpulse behavior and probabilities vary drastically between brands (as seen in Figure 3). The total probability of obtaining an afterpulse ($P(AP)$) for each detector is shown in Table I. In addition, the same table shows the time taken for the fit of the afterpulse probability to fall to 10 % ($\tau_{10\%}$) and 15 % ($\tau_{15\%}$).

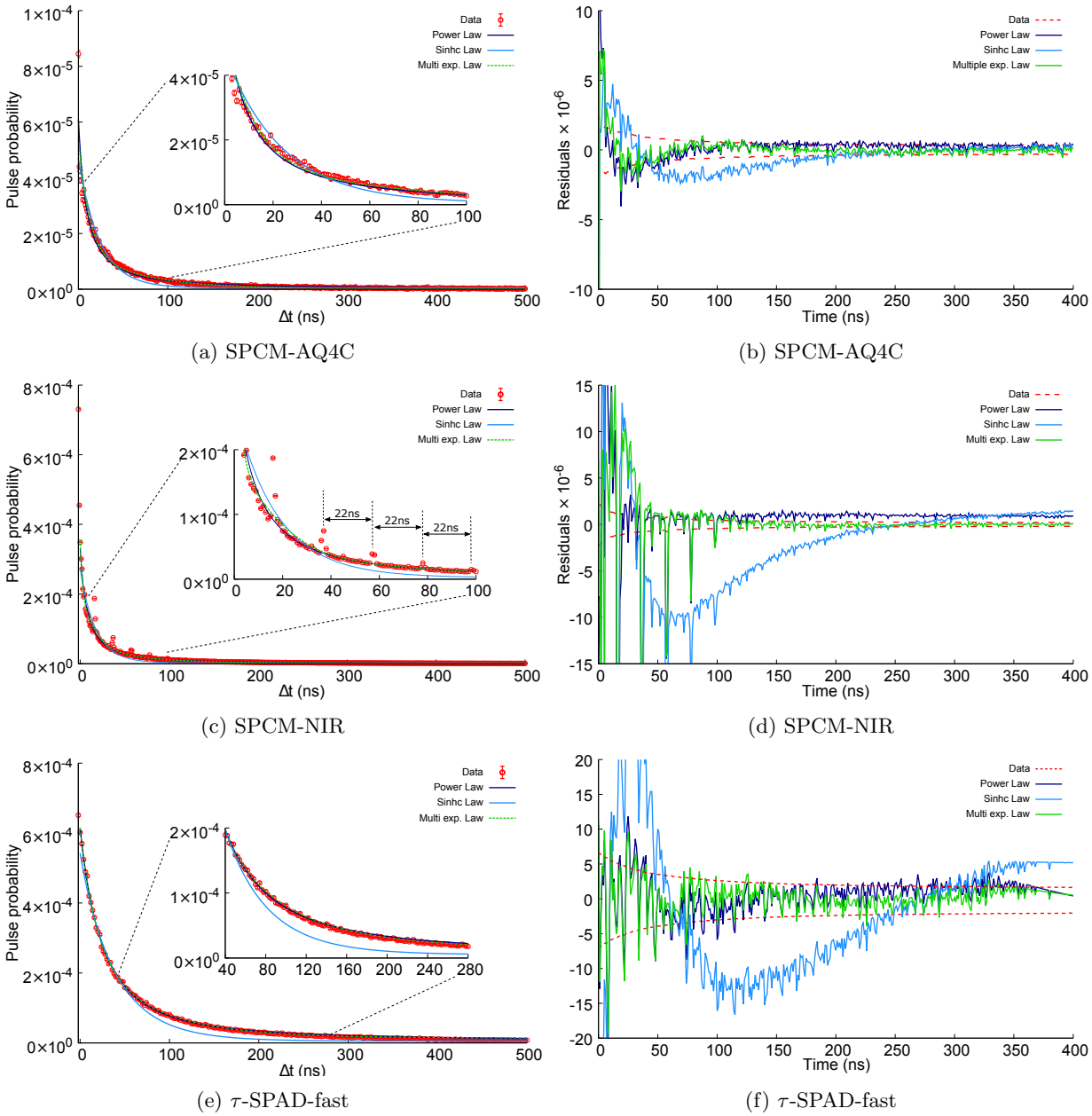

(a) SPCM-AQ4C (b) SPCM-AQ4C

(c) SPCM-NIR (d) SPCM-NIR

(e) τ-SPAD-fast (f) τ-SPAD-fast

FIG. 2: Afterpulse peak's tail fitted with Power model, Hyperbolic-sinc model and multiple exponential model for SPCM-AQ4C (PerkinElmer), SPCM-NIR (Excelitas) and τ-SPAD-fast (Laser Components) - Comparison of residuals for all detectors and models (Power model (blue), Hyperbolic sinc model (cyan) and Multiple exponential model (green)) and the red dashed lines are $\pm$ 2 standard deviation limits for statistical fluctuations. We analysed $> 0.14 \times 10^6, 2.7 \times 10^6$ and 3×10^6 *afterpulse* events for each SPCM-AQ4C, SPCM-NIR, and τ-SPAD-fast detector we analysed respectively.

B. Higher order afterpulses

Any detection event may cause an afterpulse which may induce secondary and further afterpulses which we call "higher order afterpulses". Usually afterpulsing is a small effect and the afterpulsing probability distribution function is smeared such that the higher order afterpulses are improbable. However, in the presence of strong enough twilighting[22], photon detections and afterpulses accumulate in a narrow peak that appear just after the dead time. We note this behavior in SPCM-NIR and to a lesser extent in SPCM-AQ4C, as can be seen in Figure 3. The higher order afterpulses are clearly visible as a series of peaks after the main peak with a period exactly equal to the dead time of the detector. The presence of such higher order afterpulsing was first speculated in[15] but, to

Detector	$P(AP)$ (%)	$\tau_{10\%}$ (ns)	$\tau_{15\%}$ (ns)	t_{dead} (ns)
SPCM-AQ4C	0.2854 ±0.0008	7	3	50
SPCM-NIR	1.2904 ±0.0007	8	6	22
τ-SPAD-fast	5.106 ±0.003	119	80	53

TABLE I: Table showing the total afterpulse probability ($P(AP)$), the decay time of the afterpulse to 10 % (15 %) of maximum — $\tau_{10\%}$ ($\tau_{15\%}$) and the dead time (t_{dead}) of each of the detector makes. SPCM-AQ4C Sn. 195 (2007), SPCM-NIR Sn. 29860 (2015) and τ-SPAD-fast Sn. 01019917 (2013)

the best of our knowledge, never reported.

For the SPCM-NIR, the signal pulse and the first order of afterpulse are 22 ns apart, which exactly corresponds to the duration of the dead time of this particular detector module. The measured time intervals between all following higher orders of afterpulses (as seen in the inset of the Figure 3) have the same time delay of 22 ns. We have obtained a similar plot for three detectors with the same model number: in each case, peaks appear separated by the dead time of the particular detector. Such a behavior is clearly undesirable, notably in time-resolved spectroscopy where higher order peaks could be mistaken for, or mask the true signal.

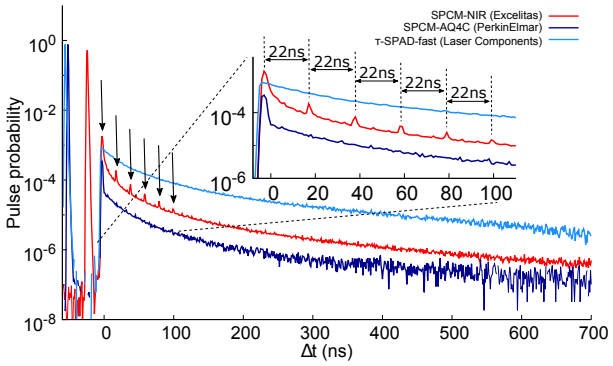

FIG. 3: $g^{(2)}$ Histograms for various detectors exhibit distinct afterpulse behavior (each afterpulse peak is marked by an arrow). For example, the τ-SPAD-fast displays an unusually gradual decay while the SPCM-NIR is the only detector make to exhibit higher order afterpulses . The inset shows the higher order afterpulses occurring at intervals equal to the dead time.

We verified that the higher order afterpulses seen are not the result of stray light, the shape of the laser pulse, electronic noise, impedance mismatch or optical reflections. We also processed the data with different bin widths and laser pulse frequencies to ensure that the observed higher order afterpulse peaks are not due to digitization noise.

Further, we note that it is possible to explain the area of the n^{th} higher order peak based on the probability of the first afterpulse ($P(AP)$) as $P(AP)^{(n+1)}$+ the probability of an afterpulse in the bin just before the n^{th} higher order peak × the number of bins in the peak. This geometric progression agrees to within 4 to 6 % for the 2^{nd} to 5^{th} order afterpulses.

C. Background and accidentals corrections during the dead time

An investigation of the region of reduced detection efficiency called the "dead-time" found between the signal pulse and the afterpulse shows yet another characteristic variation between makes of detectors, which is not part of the models used so far. In typical quantum optics experiments, there is a probability that a coincidence is detected between two different detectors erroneously, we call these coincidences "accidentals". Typically, they can be estimated from Poissonian statistics as: $r_{acc} = r_1 r_2 t_c$, where r_{acc} is the rate of the accidental counts, r_1 and r_2 are the count rates of the individual detectors and t_c is the coincidence time window used. In the duration well after a detection event, this provides a very good estimate (with a maximum variation of $\ll 3\,\%$) of the behavior. However, shortly after the detection event the detectors exhibit a "dead time" and this may be followed by an afterpulse. Many experiments simply subtract the accidental counts and this may be a good approximation when the detection rates are very low compared to the peak count rate. At high detection rates, the effect of afterpulses and the dead time become significant. In the previous sections we have characterized the afterpulse probability for several detectors. In this section we focus on the effect of the dead time.

"Dead time" is a misnomer because the detector is not completely dead/inactive instead it exhibits a reduced detection efficiency. We find that the detection efficiency is reduced by a factor α which is characteristic of the make of the detector. We use a continuous wave battery powered LED as a steady and controllable source of background illumination in addition to the attenuated laser pulses (see Figure 1). We then measured the $g^{(2)}$ histograms for different background count rates.

Detector	α_{avg}	α_{min}	α_{max}
SPCM-NIR	3.97 ± 0.06	3.86 ± 0.05	4.06 ± 0.20
τ-SPAD-fast	3.31 ± 0.06	3.30 ± 0.07	3.32 ± 0.15

TABLE II: The correction factor α to be applied for the dead time depends on the make of detector. The table shows the average value (α_{avg}) as well as the minimum (α_{min}) and maximum (α_{max}) values as the background level was varied from 40 kcps to 240 kcps. The SPCM-AQ4C is a fiber coupled detector and we could not introduce background light using the LED in the same manner as the other detectors and is hence omitted from this table.

Figure 4a shows these histograms for the SPCM-NIR while Figure 4b shows the same for the τ-SPAD-fast modules[21]. We observe that the rate of accidental coincidences (r_{acc}) between the trigger signal and the attenuated laser pulse vary linearly with the background count rate in the dead time region. We also note that the number of accidentals per bin in a region $\ll 0.7\,\mu$s away from the detection event is proportional to the number of accidentals per bin during the dead time. We call this proportionality constant α.

In the regions before the detection event, well after the detection event and even during the afterpulse, the measured accidental corrections agreed with the value calculated assuming Poissonian statistics. However, during the dead time we found that a correction of $\frac{r_{acc}}{\alpha}$ needed to be applied by subtraction. Table II shows α for different detector makes.

IV. CONCLUSION

We have clearly demonstrated that statistically significant different models are required to appropriately describe the distribution of electrical signals generated by different brands/makes of detectors. This explains the conflicting nature of several previous studies; for example[14,15,23] show strong evidence for the power model while[3,8] show equally compelling evidence for the multiple exponential model and[13] provides evidence for the hyperbolic sinc model. Recently[27] showed that the afterpulse probability is dependent on past events — a property not considered in the exponential, power, or hyperbolic sinc models. By comparing previously reported results to our own, we realize that there is a large variation between the different manufactures and makes of detectors commonly used. The suppression of afterpulses by different quenching methods[20] leads us to believe that the afterpulsing behavior is more dependent on the electronic quenching circuit used rather than the presence and distribution of discrete/continuous/quasi-continuous deep levels. This clearly proves that none of the current theoretical models are universal which makes it hard to draw conclusions about the underlying mechanism based on fundamental semiconductor physics.

We also report on the presence of higher order afterpulses in one of the tested detector models. To make this possible, unlike in several previous measurements[7,13,25] who used an auto-correlation signal, we use a cross-correlation histogram between the detector and the trigger. This allows us to look for both higher order afterpulses as well as the behavior during the dead time. These higher order afterpulses can cause large errors in measurements of the arrival times of photons and must be carefully accounted for. We were able to exclude frequency dependence in our detectors since we tested all the results shown here for several different repetition rates (all far from detector saturation) of the laser pulses ranging from 10 kHz to 1.2 MHz and found no significant variation.

Further, the total afterpulsing probability for several individual detectors all of the same manufacturer, part number, and with consecutive serial numbers varied drastically (in some cases between 5.1 and 8.5 %) implies that every individual detector needs to be calibrated for all applications that need to accurately measure count rates or arrival times of photons.

For many years, afterpulsing has been extensively studied from a semiconductor physics based perspective, where it is important to understanding how trapped charges/energy levels decay. However, to correctly study this, one must separate the effects due to the behaviour of the diode or seimiconductor junction from the effects due to the electronics and quenching circuits. For example, based on modeling the semiconductor junction, a longer dead time is thought to lead to a lower afterpulsing probability[7]. However, as seen in Table I and Figure 3 both the SPCM-AQ4C and the τ-SPAD-fast have a significantly longer dead time than the SPCM-NIR but the former has a lower afterpulse probability while the latter has a larger one. In this case it is impossible to draw a conclusion about the relationship between dead time and afterpulse probability without carefully considering the quenching circuits used. This type of analysis requires proprietary and confidential information about the diode and circuits used by the manufacturer; which is inaccessible to a typical end-user. Instead of drawing potentially erroneous conclusions about semiconductor behavior based on which model had a better fit, we focus on an application oriented perspective. For most practical purposes, it is sufficient to understand the statistical nature of the afterpulses rather than their causal mechanisms.

We also would like to mention, that we do not consider a possible aging effect of the detectors. All measurements were performed in the time span of only a few months. Commercial products, may have to be characterized repeatedly during their long operational lifetimes. The study of any aging effects on the statistical behaviour of APD's in general is an intresting avenue for further exploration.

Most applications of APDs are hindered by afterpulsing, in many cases these ill effects can be corrected for in post-processing. However, to do so one must characterize each detector individually as evidenced by the large variation in the afterpulse probabilities between detectors of the same model number, age and manufacturer under almost identical laboratory test conditions. It is possible, although inadvisable, to ignore all clicks a few hundred ns after any detection event. This effectively increases the dead time and avoids the bulk of afterpulses but this severely limits the maximum count rates and detection efficiency due to saturation-like effects. To correctly account for the ill effects of afterpulses it is sufficient to characterise each individual detector prior to/during use, using the method described in this work. Characterization methods based on the timing auto-correlation of de-

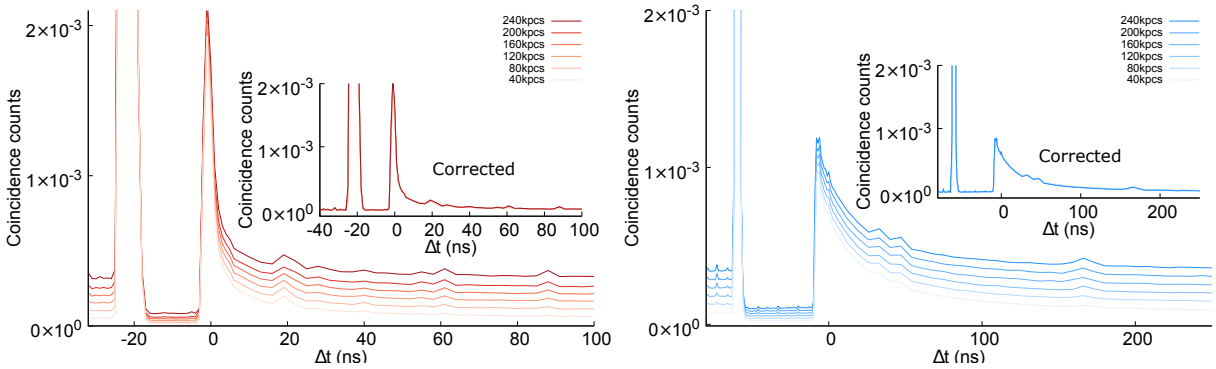

(a) Excelitas SPCM-NIR APD module.

(b) Laser Components τ-SPAD-fast APD module.

FIG. 4: $g^{(2)}$ Histograms for different background count levels, clearly showing the reduced detection efficiency in the dead time region (between the large detection peak and time $\Delta t = 0$). We observe a linear scaling of the accidental coincidences as we vary the background count rate. From which we determine a reduction factor α in this dead time region (see Table II). **Insets**: The $g^{(2)}$ histograms corrected for background counts.

tection events can easily overlook features such as higher order afterpulses and therefore should not be used.

From a quantum communication perspective, our method of characterization of every individual detector can be included into the overall device dependent security analysis[9,10]. These characterizations can also be used to improve the accuracy of results in quantum meterology.

ACKNOWLEDGEMENTS

The Authors thank FFG-ALR (contract Nr. 844360), ESA (contract Nr. 4000112591/14/NL/US) and MoSES 533-19-14-0002 as well as the Austrian Academy of Sciences for their financial support. We would like to thank Dmitri Horoshko, Vyacheslav Chizhevsky and Sergei Kilin for discussing their methods and sharing the results of their paper[13].

[1] R. G. W. Brown, K. D. Ridley, and J. G. Rarity. Characterization of silicon avalanche photodiodes for photon correlation measurements 1: Passive quenching. *Applied Optics*, 25(22):4122, 1986.

[2] M. Stipčević. A novel active quenching circuit for single photon detection with geiger mode avalanche photodiodes. *Applied Optics*, 48:1705–1714, 2009.

[3] Sergio Cova, A. Lacaita, and G. Ripamonti. Trapping Phenomena in Avalanche Photodiodes on Nanosecond Scale. *IEEE Electron Device Letters*, 12(12):685–687, 1991.

[4] Thiago Ferreira Da Silva, Guilherme B. Xavier, and Jean Pierre Von Der Weid. Real-time characterization of gated-mode single-photon detectors. *IEEE Journal of Quantum Electronics*, 47(9):1251–1256, 2011.

[5] Winfried Denk, James H Strickler, Watt W Webb, et al. Two-photon laser scanning fluorescence microscopy. *Science*, 248(4951):73–76, 1990.

[6] MD Eisaman, J Fan, A Migdall, and SV Polyakov. Invited review article: Single-photon sources and detectors. *Review of scientific instruments*, 82(7):071101, 2011.

[7] Christoph Schaeff Sven Ramelow Mario Stipčević Gerhard Humer, Momtchil Peev and Rupert Ursin. A simple and robust method for estimating afterpulsing in single photon detectors. *Journal of Lightwave Technology*, 33(14):3098–3107, 2015.

[8] A. C. Giudice, M. Ghioni, S. Cova, and F. Zappa. A process and deep level evaluation tool: Afterpulsing in avalanche junctions. In *European Solid-State Device Research Conference*, pages 347–350, 2003.

[9] Daniel Gottesman, H-K Lo, Norbert Lutkenhaus, and John Preskill. Security of quantum key distribution with imperfect devices. In *Information Theory, 2004. ISIT 2004. Proceedings. International Symposium on*, page 136. IEEE, 2004.

[10] Daniel Gottesman, Hoi-Kwong Lo, Norbert Lütkenhaus, and John Preskill. Security of quantum key distribution with imperfect devices. *arXiv preprint quant-ph/0212066*, 2002.

[11] Robert H Hadfield. Single-photon detectors for optical quantum information applications. *Nature photonics*, 3(12):696–705, 2009.

[12] Jamie Holder, RW Atkins, HM Badran, G Blaylock, SM Bradbury, JH Buckley, KL Byrum, DA Carter-Lewis, O Celik, YCK Chow, et al. The first veritas telescope. *Astroparticle Physics*, 25(6):391–401, 2006.

[13] D. B. Horoshko, V. N. Chizhevsky, and S. Ya. Kilin. Full-response characterization of afterpulsing in single-photon detectors. *arXiv:1409.6752 [quant-ph]*, pages 1–4, 2014.

[14] Mark A. Itzler, Mark Entwistle, and Xudong Jiang. High-rate photon counting with Geiger-mode APDs. *IEEE Photonic Society 24th Annual Meeting, PHO 2011*, (April 2016):348–349, 2011.

[15] Mark A. Itzler, Xudong Jiang, and Mark Entwistle. Power law temporal dependence of InGaAs/InP SPAD afterpulsing. *Journal of Modern Optics*, 59(17):1–9, 2012.

[16] Nitin Jain, Birgit Stiller, Imran Khan, Vadim Makarov, Christoph Marquardt, and Gerd Leuchs. Risk analysis of Trojan - horse attacks on practical quantum key distribution systems. 21(3), 2006.

[17] K. E. Jensen, P. I. Hopman, E. K. Duerr, E. A. Dauler, J. P. Donnelly, S. H. Groves, L. J. Mahoney, K. a. McIntosh, K. M. Molvar, A. Napoleone, D. C. Oakley, S. Verghese, C. J. Vineis, and R. D. Younger. Afterpulsing in Geiger-mode avalanche photodiodes for 1.06 μm wavelength. *Applied Physics Letters*, 88(13):10–13, 2006.

[18] Boris Korzh, Tommaso Lunghi, Kateryna Kuzmenko, Gianluca Boso, and Hugo Zbinden. Afterpulsing studies of low-noise InGaAs/InP single-photon negative-feedback avalanche diodes. *Journal of Modern Optics*, (July):1–7, 2015.

[19] David E Kuhl, Jorge R Barrio, Sung-Cheng Huang, Carl Selin, Robert F Ackermann, James L Lear, JL Wu, TH Lin, and Michael E Phelps. Quantifying local cerebral blood flow by N-isopropyl-p-[123I]iodoamphetamine (IMP) tomography. *Jour-*

nal of nuclear medicine: official publication, Society of Nuclear Medicine, 23(3):196–203, 1982.

[20] M. D. Eisaman, J. Fan, A. Migdall and S. V. Polyakov. Invited Review Article: Single-photon sources and detectors. *Acta Medica Okayama*, 67(4):259–263, 2013.

[21] We could not illuminate the SPCM-AQ4C fiber coupled detector in the same manner as the other free space coupled detectors, so we have left out these results for consistency.

[22] S. V. Polyakov and A. L. Migdall. High accuracy verification of a correlated-photon-based method for determining photoncounting detection efficiency. *Optics Express*, 15:1390–1407, 2007.

[23] Alessandro Restelli, Joshua C. Bienfang, and Alan L. Migdall. Time-domain measurements of afterpulsing in InGaAs/InP SPAD gated with sub-nanosecond pulses. *Journal of Modern Optics*, 59(August):1–7, 2012.

[24] Mario Stipčević and Daniel J. Gauthier. Precise Monte Carlo Simulation of Single-Photon Detectors. 5:1–5, 2014.

[25] Mario Stipčević, Daqing Wang, and Rupert Ursin. Characterization of a Commercially Available Large Area, High Detection Efficiency Single-Photon Avalanche Diode. *Journal of Lightwave Technology*, 31(23):3591–3596, 2013.

[26] Anja Wagner, Heiko Mahrholdt, Thomas A Holly, Michael D Elliott, Matthias Regenfus, Michele Parker, Francis J Klocke, Robert O Bonow, Raymond J Kim, and Robert M Judd. Contrast-enhanced MRI and routine single photon emission computed tomography (spect) perfusion imaging for detection of subendocardial myocardial infarcts: an imaging study. *The Lancet*, 361(9355):374–379, 2003.

[27] Fang-Xiang Wang, Wei Chen, Ya-Ping Li, De-Yong He, Chao Wang, Yun-Guang Han, Shuang Wang, Zhen-Qiang Yin, and Zheng-Fu Han. Non-Markov property of afterpulsing effect in single-photon avalanche detector. pages 18–20, 2016.

[28] Haifeng Wang, Terry B Huff, Daniel A Zweifel, Wei He, Philip S Low, Alexander Wei, and Ji-Xin Cheng. In vitro and in vivo two-photon luminescence imaging of single gold nanorods. *Proceedings of the National Academy of Sciences of the United States of America*, 102(44):15752–15756, 2005.

[29] Michael Ware, Alan Migdall, Joshua C Bienfang, and Sergey V Polyakov. Calibrating photon-counting detectors to high accuracy: background and deadtime issues. 1(1):1–13, 2006.

[30] H. T. Yen, S. D. Lin, and C. M. Tsai. A simple method to characterize the afterpulsing effect in single photon avalanche photodiode. *Journal of Applied Physics*, 104(5):1–5, 2008.

[31] We chose a value of 900 ns such that we include a significant amount of the afterpulse tail while avoiding any potential effects due to the earliest possible subsequent pulse 1 μs later.